RESEARCH PAPER

Microfluidic bolus induced gradient generator for live cell signalling

Ramesh Ramji · Partha Roy

Abstract Major events in cell biology are initiated by the binding of ligands to cell surface receptors and/or their transport into cells. We present a study of a simple microchannel system that integrates a bolus generator and surface-adhered cell culture domains. Our system allows the delivery of small packets or boluses of biomolecules to a cell population. Owing to pressure driven microfluidic flow of the bolus, a gradient of cell surface bound ligands is established along the length of the microchannel. Experimental data for the epidermal growth factor (EGF) binding to its receptor on A431 cells are presented. We highlight the effect of changing Peclet number (or flowrate), bolus shape, bolus volume and ligand concentration on the gradient formed longitudinally in the microchannel. A mathematical model describing the transient convection, diffusion, dispersion and binding of ligands to cell surface receptors is developed. The model provides essential design guidelines for our system with good qualitative agreement with experimental data. The results suggest ways to modulate the amount of bound ligand and the gradient independently. This simple microsystem is suitable for generating longer range gradients involving larger cell populations as compared to existing microfluidic systems.

Abbreviations

EGF	Epidermal growth factor
EGFR	Epidermal growth factor receptor
PDMS	Polydimethylsiloxane
DMEM	Dulbeccos modified eagles medium
ATCC	American type culture collection
BIGG	Bolus induced gradient generator

R. Ramji and P. Roy are contributed equally to this article

R. Ramji · P. Roy (✉)
Department of Bioengineering, National University of Singapore, Singapore 117576, Singapore
e-mail: partha714.pr@gmail.com

1 Introduction

The role of biomolecular gradients in inducing events like development, migration and differentiation in cells has been recognized and is an active area of research (Baier and Bonhoeffer 1992; Gurdon and Bourillot 2001; Keenan and Folch 2007; Singh et al. 2008). Different levels of biomolecular availability, to implement signalling over varied lengths in vivo, are seen in paracrine and endocrine signalling pathways (Luciano et al. 1990; Balla 2006). Relative changes in these signalling pathways alter the spatial range of signal communication by varying the amount of triggered ligand–receptor complexes, resulting in system disorders (Spiegel 1996; Kahn and Flier 2000; Manji and Lenox 2000; Singh and Harris 2005). Earlier in vitro studies were hampered by the lack of precision of the gradient generation methods (Keenan and Folch 2007; Khademhosseini 2008). More recently, the advent of microfluidics technology has enabled important questions in cell biology to be addressed by imposing precisely controlled gradients of analytes on a cell population (Folch

and Toner 2000; Beebe et al. 2002; Holmes and Gawad 2010). Many steady state (passive) and flow-based methods of establishing biomolecular gradients, for cell based studies within microdevices have been described and reviewed earlier (Keenan and Folch 2007; Khademhosseini 2008). Although many of these methods form stable concentration gradients along the channel width (Dertinger et al. 2002; Li Jeon et al. 2002; Saadi et al. 2006; Okuyama et al. 2010; Tan et al. 2010), they not only require continuous supply of analytes but also restrict the study of cellular effects to relatively shorter length scales (typically < 1 mm) and smaller cell numbers.

Methods which generate biomolecular gradients over a longer length scale (few cm) within a microdevice have been described recently by a few research groups (Goulpeau et al. 2007; Du et al. 2008, 2010; Kang et al. 2008; Seidi et al. 2011; Sackmann et al. 2012). The method followed by Goulpeau et al. (2007) produce a longitudinal concentration gradient using microvalves controlling transient dispersion along the flow while that by Du and co-workers (2008) use a passive pump induced forward flow which does not require the use of syringe pumps. Although these methods offer some advantages, they either use microvalves that make fabrication difficult or use a passive pump based approach where the system lacks perfusion over the period of gradient generation (Du et al. 2008; Seidi et al. 2011). In addition, these studies are concerned with the generation of stable extracellular gradients of biomolecules instead of gradients of cell surface bound molecules.

A few methods of producing cell surface or ECM bound biomolecular gradients have been reported for growth cone and neuronal guidance related studies (Tessier-Lavigne and Goodman 1996; Dertinger et al. 2002; Adams et al. 2005; Millet et al. 2010; Sackmann et al. 2012). Joanne et al. developed a valve-based composite gradient generator to produce diffusible and surface bound guidance cues. Surface bound N-shaped laminin gradient was produced to study the changes in polarity of growth cone responses to mean concentration gradients of solubilized brain derived neurotrophic factors (Wang et al. 2008). Photo-immobilization of peptides allowed precise control of surface bound gradients (Adams et al. 2005). Other approaches for producing pre-patterned surface bound laminin gradients on glass coverslips were demonstrated using principles of laminar flow, diffusion and physisorption (Dertinger et al. 2002; Millet et al. 2010). Although these studies demonstrated methods to produce substrate bound or patterned gradients, they did elucidate methods which control and generate live, cell surface bound biomolecular gradients.

A few researchers have produced plugs of molecules within a microfluidic device (Bai et al. 2002; Walker and Beebe 2002; Wu et al. 2004; Filipowicz-Szymanska 2008). Bai and co-workers (2002) developed a pressure-pinched

injection method to produce nanolitre volume of plugs within a microfluidic device using microvalves. Verpoorte et al. (Filipowicz-Szymanska 2008) demonstrated the application of Bai's method of pressure pinched-injection, on a monolithic column in a microchannel. However, these studies did not incorporate any live cells and thus, did not quantify the bound molecules.

In this paper, we establish transient gradients of bound or internalized molecules using a 'bolus' or small packet of the biomolecule which is transported over a cell population. Here, we demonstrate for the first time, a simple method to generate live cell surface bound ligand gradients by injecting a bolus into a straight microchannel. Our method of generating a bolus involves direct injection of a small volume of fluid (200 nL) into the channel with the help of a syringe pump. The bolus induced gradient generator (BIGG) is a novel platform which is robust and can establish short and long range ligand gradients on cells rapidly. We demonstrate this method with a well-studied ligand-receptor system, i.e., epidermal growth factor receptor (EGF-EGFR) (Sako et al. 2000). The EGF binds to EGFR on A431 epidermoid carcinoma cell line, which is well known to over express EGFR's (Yoshimoto and Imoto 2002). An accompanying mathematical model describes the transport and binding of EGF to EGFR and provides essential design guidelines.

2 Theory

2.1 Model formulation

The physical system depicted in Fig. 1a comprises a straight length of microfluidic channel with rectangular cross-section. The designated area of the microchannel contains the cultured cells. A bolus containing the ligand is injected at the start ($t = 0$) of the experiment and travels the length of the microchannel at an average velocity (U_a) while undergoing dispersion, diffusion and ligand depletion by binding to cell surface receptors. The ligand concentration in the bolus, C, changes transiently as the bolus travels along the length of the microchannel due to ligand binding to the cell surface receptors. The governing mass balance equation for the ligand may be written in dimensionless form as:

$$\frac{\partial C}{\partial t} + U(z)\frac{\partial C}{\partial x} - \frac{1}{Pe_D}\frac{\partial^2 C}{\partial x^2} - \frac{\lambda}{Pe_m}\frac{\partial^2 C}{\partial z^2} = 0. \qquad (1)$$

where C is made dimensionless with inlet concentration C_0, x with length (L), z with height (H) and time (t) with L/U_a, $\lambda = L/H$, U_a is average velocity and $U(z)$ is made dimensionless with U_a. Ligand diffusivity is D_m and dispersion is D_s giving the following mass transfer Peclet numbers,

Fig. 1 **a** A schematic representation (*side view*) of a bolus flowing inside a microchannel of dimensional length (L) and height (H) is shown. A monolayer of cells expressing surface receptors are specifically bound by fluorophore conjugated ligands. **b** A schematic representation of the optical and fluidic pathways for the bolus induced gradient generator. *Dimensions mentioned in the figure are in mm*
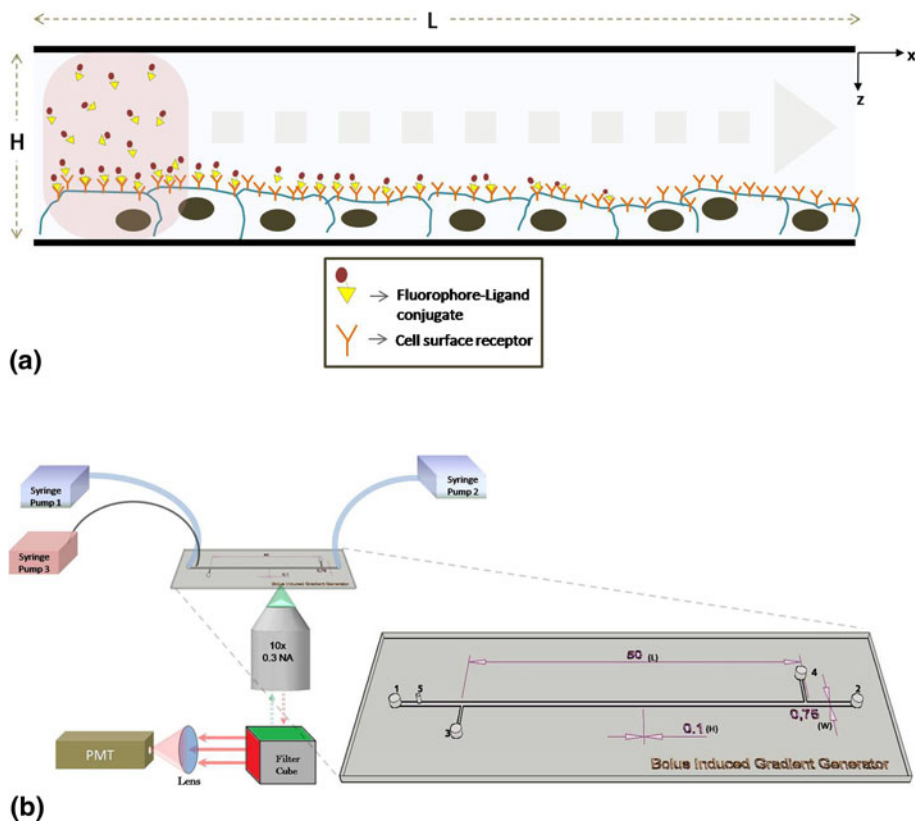
$$Pe_D = \frac{U_a L}{D_S}, \text{ and } Pe_m = \frac{U_a H}{D_m}.$$

Equation (1) is subjected to the following initial and boundary conditions at

$$t = 0, \text{ all } x \text{ and } z : C = 0 \tag{2a}$$

$$z = 1, t > 0, \text{ all } x : \frac{\partial C}{\partial z} = -Sh(C - C_{LW}) \tag{2b}$$

$$z = 0, t > 0, \text{ all } x : \frac{\partial C}{\partial z} = 0 \tag{2c}$$

$$x = 0, \text{ all } z : C - \frac{1}{Pe_D}\frac{\partial C}{\partial x} = 1 \, (0 \leqslant t \leqslant t_b) \text{ or } 0 \, (t > t_b),$$

ideal bolus shape $\tag{2d}$

$$x = 1, t > 0, \text{ all } z : \frac{\partial C}{\partial x} = 0 \tag{2e}$$

where $Sh = \frac{K_0 H}{D_m}$, with K_0 as a mass transfer coefficient.

The binding to cell surface receptors may be described by two additional equations, one for free ligand (C_{LW}) and one for bound ligand (C_{RL}) as follows

$$\frac{dC_{LW}}{dt} = a[C - C_{LW}] - b_1 C_{LW}[C_{R0} - C_{RL}] + b_2 C_{RL} \tag{3a}$$

$$\frac{dC_{RL}}{dt} = b_1 C_{LW}[C_{R0} - C_{RL}] - b_2 C_{RL} \tag{3b}$$

where

$$a = \frac{K_0 S L}{V U_a}; \; b_1 = \frac{k_f C_0 L}{U_a}; \; b_2 = \frac{k_r L}{U_a},$$

C_{LW} represents the solution phase free ligand concentration in an infinitesimally thin layer on the cell surface. C_{RL} is the bound ligand concentration which is converted to a superficial (volume basis) concentration. Concentrations are made dimensionless with respect to the inlet concentration C_0. S is cell occupied surface area, $V = SH$, the association (k_f) and dissociation (k_r) kinetic rate constants, C_{R0} is the dimensionless superficial total receptor concentration. Equations (3a) and (3b) are coupled to Eq. (1) via Eq. (2b) since C in Eq. (2b) and Eq. (3a) is identical. The length of the bolus at the inlet is expressed as a function of time. The time is made dimensionless with total channel length L, hence $t_b L$ is the dimensional length of the bolus at the inlet.

2.2 Numerical solution

Equation (1) coupled to Eqs. 3a and 3b were solved in COMSOL multiphysics v3.5a using the convection diffusion module by direct PARDISO solver. Extremely fine mesh of the entire domain containing 10,000 elements was used to avoid numerical instabilities arising at the inlet ($x = 0$). The numerical results were verified by comparison with analytical or numerical results for the special cases of,

(1) no binding and dispersion (Roy 2008), and (2) no binding (Brenner 1962). All simulations were carried out on a Laptop PC with a 2.53 GHz Intel Pentium CPU and 4 GB of RAM.

3 Materials and methods

Most of the materials were purchased from Sigma Aldrich Singapore, unless otherwise stated.

3.1 Microfluidic device fabrication

The *BIGG* was fabricated using polydimethylsiloxane, PDMS (Sylgard 184, Dow Corning, USA) following conventional rapid prototyping and soft lithography techniques (Tan et al. 2010). Briefly, an 8 inch photomask containing an array of 65 mm $(L) \times 0.75$ mm $(W) \times 0.1$ mm (H) channels was printed on a plastic sheet using commercial photo plotting direct write laser imagers at 50,000 dpi resolution. A silicon master with positive relief features was fabricated using a negative photoresist (SU-8 2035, MicroChem Co, USA) following standard photolithographic techniques.

Prior to the soft lithography step and to prevent undesired bonding of PDMS to the master, the silicon master was silanized with Trichloro(1H,1H,2H,2H-perfluorooctyl)silane in a desiccator for 15 min at room temperature. A mixture of PDMS-prepolymer and curing agent (10:1 ratio) was poured over the master, degassed to remove bubbles and then cured overnight at 65 °C. The cured PDMS molds were peeled away from the master and cut to the size of standard glass slides $(25 \times 75$ mm). Channel inlets and outlets (Fig. 1b) were punched using 1.5 mm diameter Harris Uni-Core™ puncher (Ted Pella Inc, USA). Following the inlets and outlets, another hole was punched a few millimetres away from the main inlet, right in the middle of the channel using a 0.5 mm diameter Harris Uni-Core™ puncher, to facilitate the injection of bolus. The PDMS mold was then cleaned and rinsed with isopropyl alcohol, de-ionized water and blow dried to remove traces of solvents. Succeeding the cleaning steps, the PDMS mold was bonded permanently to a 25×75 mm, glass coverslip (Electron Microscopy Sciences, USA) by subjecting both of them to oxygen plasma for 30 s at 200 W radio frequency generator power and 450 mTorr oxygen pressure (March Instrument Incorporated, USA). An irreversible seal between the surface of the PDMS containing the microchannel and the glass cover slip was formed by sandwiching both the surfaces together, soon after the plasma treatment and further incubating them for 4 h at 65 °C.

3.2 Cell culture

A431 cells from American type culture collection (Manassas, USA) were cultured in DMEM supplemented with 4.5 g/L glucose, 4 mM L-glutamine, phenol red (Hyclone, USA), 1 mM sodium pyruvate, 10 % FBS (Hyclone, USA), 50,000 IU/L penicillin and 50 mg/L streptomycin. Cells were grown at 37 °C in a humidified incubator maintained at 5 % CO_2 in standard T-25, tissue culture flasks.

Once the cells were 95 % confluent, they were trypsinized with $2\times$ 0.5 % Trypsin–EDTA (Caisson Labs, USA), centrifuged and re-suspended in DMEM complete medium to a count of 4.3 million cells/mL. Prior to cell seeding inside the BIGG platform, the microdevice was subjected to oxygen plasma treatment for 15 min (Harrick Plasma Cleaner, USA) to render the surface of the channels more hydrophilic, thus creating a suitable environment for the cells to attach and proliferate (Zhou et al. 2010). Inlet 5 was temporarily sealed with a transparent scotch tape following which the channel was perfused with the cell culture medium through inlet 3, without any bubble formation within the channels. Once the holes 1, 2 and 4 were completely filled with medium, holes 1 and 2 were blocked using stoppers. A volume of 100 μL cell suspension at the aforementioned cell density was perfused from inlet 3 and allowed to pass through outlet 4 with micropipettes placed at both the ends acting as a source and a sink. The BIGG microdevice was then incubated at 37 °C inside a 5 % CO_2 incubator and was left undisturbed for a period of 12 h to allow the cells to attach at the bottom of the channel. After the 12 h incubation period, the cells were constantly perfused with cell culture media and were allowed to grow inside the channel to become >95 % confluent inside the 50×0.75 mm seeding area.

3.3 Bolus generation

The microdevice was placed on the microscope stage (Nikon TE2000U fluorescence microscope) that was preset to 37 °C with the help of a stage heater. FEP tubings (1/32″ id, Cole-Parmer, USA) connecting the microdevice were plasma treated to render their inner walls clean to avoid air bubbles while priming them with media without phenol red. Inlet 1 and outlet 2 were connected to two syringe pumps (KD Scientific and Cole-Parmer, USA), which were maintained at the same injection and withdrawal rate, respectively, while inlet 3 and outlet 4 were blocked with stoppers. The bolus injection system included a 250 μL Hamilton syringe with a long stainless steel cannula placed on another syringe pump (New Era Pump Systems Inc., USA). Boluses of desired volumes were injected into the channel through inlet 5 after priming the cannula

Fig. 2 Fluorescence photomicrograph of a 200 nL bolus containing 0.1 mM rhodamine dye, travelling through the BIGG microchannel. The bolus clearly forms a double parabola, where **a** depicts the frontal region and **b** shows the tail of the bolus. **c** A normalized intensity versus time (*dimensionless*) profile showing three repeats (*black circle*, *green square*, *red triangle*) of a 200 nL bolus containing 50 nM EGF-TMR conjugate travelling with a velocity of 0.0222 cm/s. The intensity is normalized with the maximum intensity while the time is normalized with the residence time (L/U_a) of the bolus within the channel. The bolus width is determined at 20 % of the maximum normalized intensity
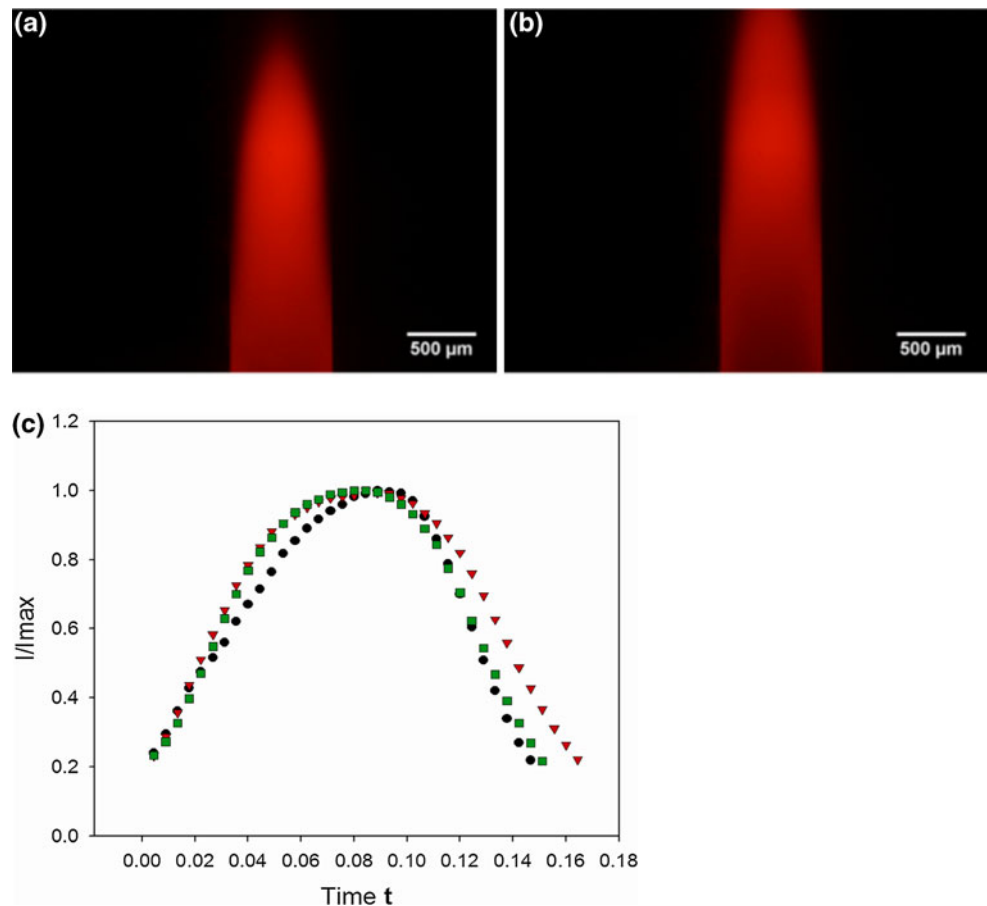
completely and inserting it into the inlet by removing the scotch tape. Pumps controlling the flow of cell media (without phenol red) inside the main channel were stopped temporarily at the time of bolus injection and were resumed once the bolus was completely injected into the microchannel (see Fig. 2a, b).

3.4 Optical detection

Fluorescence measurements were done with a $10\times$ 0.3 NA (CFI Plan Fluor, Nikon) objective. Images of cells stained with respective fluorescent ligands were captured with DXM1200C (Nikon) CCD camera. Excitation and emission of epidermal growth factor fluorescent tetramethyl rhodamine conjugate (EGF-TMR) (Invitrogen, Life Technologies, Singapore) was carried out with a filter cube containing 510–560 nm BP (Ex), 575 nm DM and 590 nm (Em) LP filters. Fluorescence intensities over the channel length were measured using a photon counting head (Hamamatsu, Japan). Mercury lamp intensity fluctuations were minimal (≈ 2.78 %) over the period of intensity measurement. Photobleaching effects were negligible (≈ 0.7 % change in 45 s) during measurements as standard protocols from previous studies in our laboratory were

followed, appropriately. Background intensities were first measured at selected points over the channel length followed by bolus injection. Fluorescence intensities at the same points were measured immediately after the bolus passed through the channel. Non-specific binding of EGF-TMR to the microchannel was negligible since the intensity dropped back to baseline in the cell free area after the bolus transit. Bright field as well as fluorescent images of cells was processed using ImageJ software. Statistical analysis of all experimental data was carried out with the two sample student t test, assuming equal variances (unpaired) with significance at $p < 0.05$.

4 Results and discussion

This study is conducted in a single rectilinear microchannel with a rectangular cross-section (see Fig. 1b) comprising (1) a short initial section devoid of cells, where the bolus is injected and flow profile established, and (2) a longer section with surface attached cells, where the ligand binding and subsequent imaging occurs. The mathematical model describes the section containing cells by quantifying the bound ligand (experimentally quantified by

Table 1 A list of parameter values applied in the numerical calculations presented in Figs. 3, 4, 5, 6, and 7

Parameter	Numerical value
D_m (EGF) (Thorne et al. 2004)	12.9×10^{-7} cm²/s
D_S	Equation given in Rush et al. (2002)
Total number of receptors/cell (Felder et al. 1992)	1.8×10^6
Total number of cells in confluent monolayer	88,650
Kinetic association rate constant (k_f) (Felder et al. 1992)	$1.2 \pm 5.6 \times 10^7$ M⁻¹s⁻¹
Kinetic dissociation rate constant (k_r) (Felder et al. 1992)	$1.6 \pm 0.2 \times 10^{-3}$ s⁻¹
Cell covered length (L)	50 mm
Cell covered width (W)	0.75 mm
Height (H)	0.1 mm
Mass transfer coefficient (K_0) (Model and Omann 1995)	8.87×10^{-3} cm/s

Fig. 3 The effect of bolus shape on the gradient formed. Numerical results for the normalized bound ligand concentration is plotted against the dimensionless length for a 200 nL bolus volume, $C_0 = 50$ nM and Ua = 0.0222 cm/s. *Dotted line* (*black*) represents a double parabola while the *long dash* (*red*) represents the ideal square shaped bolus
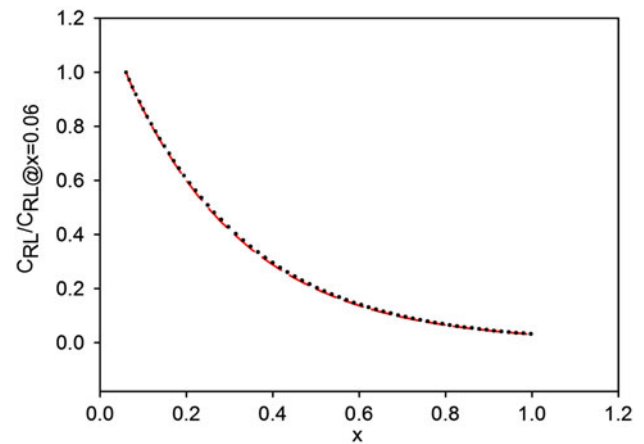
fluorescence imaging). All numerical results are based on the parameter values given in Table 1. Experimental results are presented for the convection dominated high Peclet number regime ($150 < Pe_m < 550$), illustrating, inter alia, the effect of the most easily varied bolus properties such as volume and concentration of ligand.

4.1 Effect of bolus shape

The ideal starting shape of the bolus is a cuboidal plug. However, the shape observed to form experimentally is similar to a double parabola (see Fig. 2a, b). This parabolic shape is seen across the microchannel width, while the shape along the height is unknown as it is difficult to image. For the purpose of our 2D model, we compared the ideal bolus shape with that of the double parabola. A 3D model would not increase the numerical accuracy since the exact shape along the height is unknown. Figure 3 shows that the slope of the normalized bound ligand versus longitudinal distance curve ($Pe_m = 172$) is identical for the parabolic and plug bolus (except for the entrance region $x < 0.05$, not shown in Fig. 3, where the slopes differ) shapes. However, the absolute value of bound ligand is higher for the plug bolus shape due to the shorter transport distance to the cell surface.

4.2 Variability between cell populations

Experimental data presented in Fig. 4 shows the difference in normalized bound ligand gradient between cell populations when all other parameters are fixed including a Pe_m of 172. The differences are most pronounced at $x < 0.4$ and
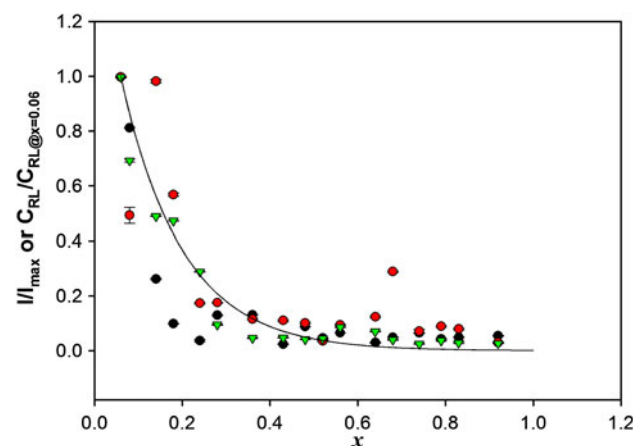
Fig. 4 Bound ligand gradient variation with cell population. Three cell populations (*red triangle*, *green circle* and *black circle*) subjected to a 50 nM, 200 nL EGF-TMR bolus, $U_a = 0.0222$ cm/s. Data are represented as normalized intensity mean plotted against normalized length with a standard deviation estimated from six consecutive intensity measurements. *Solid line* represents the model prediction

much reduced further downstream. The numerical result given in Fig. 4 predicts a similar gradient to that observed experimentally. Within the constraints of the approximate parameter values given in Table 1, there is a good qualitative agreement between model and experiment.

4.3 Effect of Peclet number (or flowrate)

The flowrate or Peclet number (Pe_m) is an important operating parameter that may be used to modulate the gradient of the bound ligand curve. Although, a change in flowrate has multiple effects on the transport of nutrient
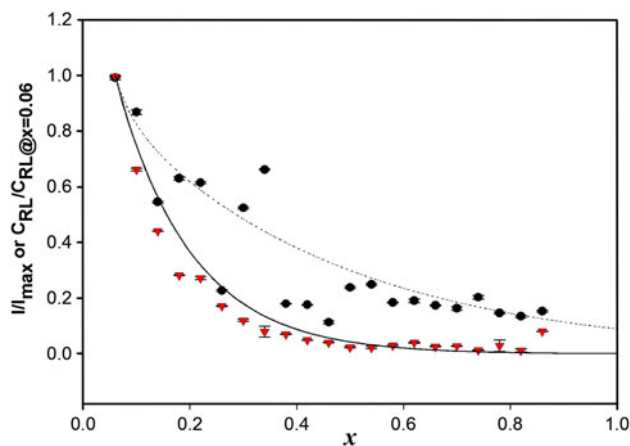
Fig. 5 Effect of Peclet number or flow rate on the gradient formed. The data points represent a 200 nL bolus containing 50 nM EGF-TMR conjugate perfused at $U_a = 0.0222$ cm/s (*red triangle* experiment, *solid line* model) and $U_a = 0.0666$ cm/s (*filled circle* experiment, *dashed line* model). Experimental data are represented as normalized intensity mean for six consecutive intensity measurements plotted against normalized length
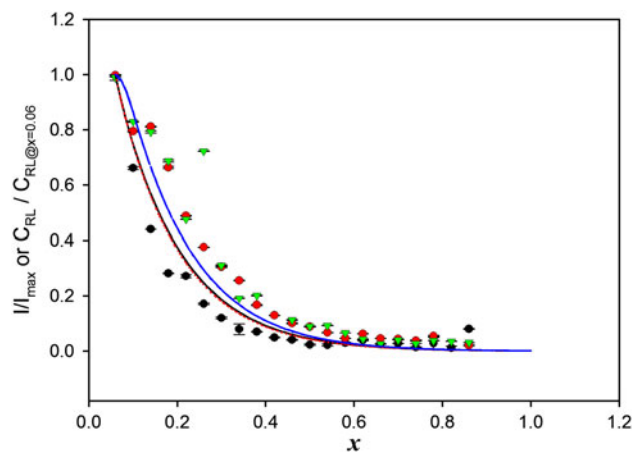

Fig. 6 Effect of ligand concentration on the gradient formed. The data points represent a 200 nL bolus travelling at $U_a = 0.0222$ cm/s containing EGF-TMR conjugates of $C_0 = 50$ nM (*black circle* experiment, *dotted red line* model), $C_0 = 150$ nM (*red diamond* experiment, *black solid line* model) and $C_0 = 300$ nM (*green triangle* experiment, *blue dashed line* model). Experimental data are represented as normalized intensity mean for six consecutive intensity measurements plotted against normalized length

molecules and shear stress exerted on cells, the transient nature of the bolus transport should allow this gradient modulation to be carried out without an adverse effect on the cells. Experimental data in Fig. 5 show a statistically significant difference in the bound ligand gradient as Peclet number changes from 172 ($U_a = 0.022$ cm/s) to 516 ($U_a = 0.066$ cm/s). This is well supported by the numerical results with a good agreement between model and experiment in Fig. 5. Nevertheless, the absolute amount of bound ligand is higher for lower Peclet number due to the fact that the residence time increases as flow velocity reduces, allowing more ligands to bind to unoccupied receptors. Surface plots representing the change in the ligand concentration during the bolus transit in the microchannel are given in supplementary Fig. 4.

4.4 Effect of initial ligand concentration

The concentration of ligand in the injected bolus is another adjustable experimental parameter. It is important to understand how this parameter influences the gradient formed. The numerical result shown in Fig. 6 is interesting as it suggests that the gradient remains unchanged over a range of concentrations, i.e., below the receptor saturation limit (see discussion on bolus volume for mole numbers). However, the absolute amount of bound ligand increases with increasing concentration as expected. Experimental data in Fig. 6 show statistically insignificant difference in gradient between the 150 and 300 nM boluses. However, the gradient observed for 50 nM is statistically significant when compared to 150 or 300 nM. Although the normalized numerical data show similarity between 50 and

150 nM concentrations, they differ in the absolute values of bound ligands at the initial part of the channel.

4.5 Effect of bolus volume

The volume of bolus injected was fixed at 200 nL for Figs. 4, 5, and 6 as it gave rise to an appropriate bolus length (see Fig. 2c) of about 15 % of the cell covered microchannel length. Typical values of the bolus length are expected to range from 2 to 20 % of the total cell covered length. Longer length boluses may also be suitable for certain experimental conditions and Fig. 7 highlights the effect of changing bolus volume. The numerical result shows that an increase in bolus volume from 200 to 600 nL (length increases from 15 to 45 % of total length) at a fixed ligand concentration of 50 nM will not change the bound ligand gradient significantly although the absolute value of bound ligand will be higher for the larger volume bolus. Note that the total moles of ligand are different in the two bolus volumes changing from 14 femtomoles to 42 femtomoles (total moles of receptor as per Table 1 data are about 100 femtomoles). The corresponding experimental data are in close agreement with this model prediction.

It is worthwhile to consider the observed quantitative difference between the model prediction and experimental data in Figs. 4, 5, 6, and 7. It is observed that the value of the mass transfer coefficient for any given ligand plays an important role in acquiring a quantitative fit. The results reported in this work have been obtained using a K_0 value as reported in Table 1. Model and Omann (1995) suggest that the value of the mass transfer coefficient for any ligand
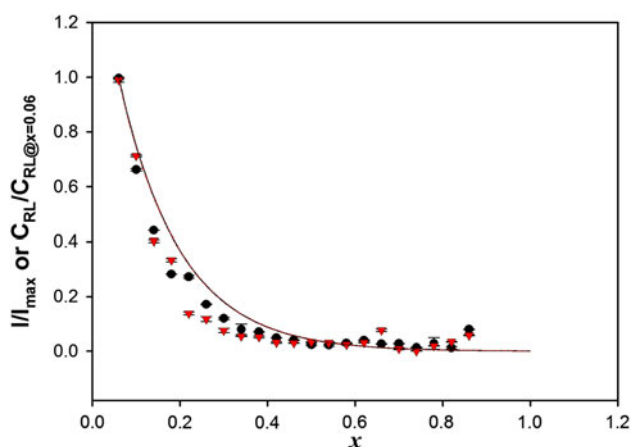
Fig. 7 Effect of bolus volume on the bound ligand gradient. The data points represent a bolus containing 50 nM EGF-TMR conjugate travelling at $U_a = 0.0222$ cm/s with volumes of 200 nL (*black circle* experiment, *black solid line* model) and 600 nL (*red triangle* experiment, *red dotted line* model). Experimental data are represented as normalized intensity mean for six consecutive intensity measurements plotted against normalized length

binding system lies in the range of the product of the association rate constant and the surface receptor density per cell. Considering this for EGFR expression on A431 cells, the value of K_0 would likely be in the range of $8–9 \times 10^{-3}$ cm/s, providing a better agreement with experimental data. It may be noted that an increase in K_0 will shift the normalized bound ligand curve to the left and a decrease in K_0 will shift the curve to the right. One may also choose to estimate the value of the mass transfer coefficient, for a given ligand-receptor pair, using similar experimental systems. This approach is expected to yield the best quantitative agreements between model and experiment.

A number of important questions may be posed about the bound ligand gradient generated by application of a bolus as described here. One question involves the total moles of ligand, i.e., what is the outcome of different ligand concentrations and bolus volumes such that the total initial moles of ligand injected remain fixed. This is answered by statistical comparison of experimental data given in Figs. 6 and 7. Comparing the bolus of volume 200 nL and C_0 of 150 nM with the bolus of volume 600 nL and C_0 of 50 nM ($Pe_m = 172$), a statistically significant difference (about 90 % of the points) of bound ligand gradient is observed. Another question that addresses the specific nature of the cellular response to the bound ligand is whether one can independently modulate the absolute value of the bound ligand and its gradient. Clearly, the results presented in Fig. 6 suggest that this is possible and thereby allows additional insight to be gained.

The BIGG platform also allows generation of multiple gradients by injecting different biomolecules one at a time

into a single inlet at the initial part of the channel or by injecting two different biomolecules from two separate inlets present on either sides of the channel as subjective to the channel design. The former method would help to generate multiple unidirectional gradients while the latter method would help to generate bi-directional gradients. One might also be able to achieve multiple gradients simultaneously by injecting a bolus containing a mixture of biomolecules. Based on the apparent binding rates of these biomolecules and also parameters such as concentration, flow velocity and volume of bolus, one may employ similar models to predict the profiles of the multiple gradients.

5 Conclusion

A simple microchannel system, integrating a bolus generator with surface adherent cells, is presented. This system is especially suited to generate transient gradients of cell surface receptor bound or internalized ligands. An accompanying mathematical model describing the transport and binding of a biomolecule or ligand yields good qualitative agreement with the experimental data of averaged intensity from cell surface bound fluorescent ligand. This method may be easily extended to generate multiple gradients of biomolecules over a cell population, for the study of cell response under well-controlled conditions. In addition, the BIGG platform allows one to study effects in cell–cell communication by creating stimulated receptor gradients of varying length scale among cells inside a microchannel. Integrating this simple device with other microsystems is expected to yield a powerful tool for biological research and other specific applications.

References

Adams DN, Kao EYC et al (2005) Growth cones turn and migrate up an immobilized gradient of the laminin IKVAV peptide. J Neurobiol 62(1):134–147

Bai X, Lee HJ et al (2002) Pressure pinched injection of nanolitre volumes in planar micro-analytical devices. Lab Chip 2:45–49

Baier H, Bonhoeffer F (1992) Axon guidance by gradients of a target-derived component. Science 255(5043):472–475

Balla T (2006) Phosphoinositide-derived messengers in endocrine signaling. J Endocrinol 188(2):135

Beebe D, Wheeler M et al (2002) Microfluidic technology for assisted reproduction. Theriogenology 57(1):125–135

Brenner H (1962) The diffusion model of longitudinal mixing in beds of finite length. Numerical values. Chem Eng Sci 17:229–243

Dertinger SKW, Jiang X et al (2002) Gradients of substrate-bound laminin orient axonal specification of neurons. Proc Natl Acad Sci 99(20):12542

Du Y, Shim J et al (2008) Rapid generation of spatially and temporally controllable long-range concentration gradients in a microfluidic device. Lab Chip 9(6):761–767

Du Y, Hancock MJ et al (2010) Convection-driven generation of long-range material gradients. Biomaterials 31(9):2686–2694

Felder S, LaVin J et al (1992) Kinetics of binding, endocytosis, and recycling of EGF receptor mutants. J cell biol 117(1):203–212

Filipowicz-Szymanska A, Rosenling T et al (2008) Pressure-pinched injection in PDMS microchips containing in situ prepared monolithic phases. In: Twelfth International Conference on Miniaturized Systems for Chemistry and Life Sciences, San Diego, California, USA, 12–16 Oct 2008

Folch A, Toner M (2000) Microengineering of cellular interactions. Annu Rev Biomed Eng 2(1):227–256

Goulpeau J, Lonetti B et al (2007) Building up longitudinal concentration gradients in shallow microchannels. Lab Chip 7(9):1154–1161

Gurdon JB, Bourillot PY (2001) Morphogen gradient interpretation. Nature 413(6858):797–803

Holmes D, Gawad S (2010) The application of microfluidics in biology. Methods Mol Biol 583:55–80

Kahn BB, Flier JS (2000) Obesity and insulin resistance. J Clin Invest 106(4):473–481

Kang T, Han J et al (2008) Concentration gradient generator using a convective–diffusive balance. Lab Chip 8(7):1220–1222

Keenan TM, Folch A (2007) Biomolecular gradients in cell culture systems. Lab Chip 8(1):34–57

Khademhosseini A (2008) Micro and nanoengineering of the cell microenvironment: technologies and applications. Artech House Publishers, London

Li Jeon N, Baskaran H et al (2002) Neutrophil chemotaxis in linear and complex gradients of interleukin-8 formed in a microfabricated device. Nat Biotechnol 20(8):826–830

Luciano SD, Vander AJ et al (1990) Human physiology—the mechanisms of body function. Mcgraw-Hill, Inc., New York

Manji HK, Lenox RH (2000) Signaling: cellular insights into the pathophysiology of bipolar disorder. Biol Psychiatry 48(6):518–530

Millet LJ, Stewart ME et al (2010) Guiding neuron development with planar surface gradients of substrate cues deposited using microfluidic devices. Lab Chip 10(12):1525–1535

Model MA, Omann GM (1995) Ligand-receptor interaction rates in the presence of convective mass transport. Biophys J 69(5):1712–1720

Okuyama T, Yamazoe H et al (2010) Cell micropatterning inside a microchannel and assays under a stable concentration gradient. J Biosci Bioeng 110(2):230–237

Roy P (2008) Measurement of Translational Diffusivity by Microchannel Multiphase Flow. J Biomech Sci Eng 3(3):380–389

Rush BM, Dorfman KD et al (2002) Dispersion by pressure-driven flow in serpentine microfluidic channels. Ind Eng Chem Res 41(18):4652–4662

Saadi W, Wang SJ et al (2006) A parallel-gradient microfluidic chamber for quantitative analysis of breast cancer cell chemotaxis. Biomed Microdevices 8(2):109–118

Sackmann EK, Berthier E et al (2012) Microfluidic kit-on-a-lid: a versatile platform for neutrophil chemotaxis assays. Nature 410(6824):50–56

Sako Y, Minoghchi S et al (2000) Single-molecule imaging of EGFR signalling on the surface of living cells. Nat Cell Biol 2(3):168–172

Seidi A, Kaji H et al (2011) A microfluidic-based neurotoxin concentration gradient for the generation of an in vitro model of Parkinson's disease. Biomicrofluidics 5:022214

Singh AB, Harris RC (2005) Autocrine, paracrine and juxtacrine signaling by EGFR ligands. Cell Signal 17(10):1183–1193

Singh M, Berkland C et al (2008) Strategies and applications for incorporating physical and chemical signal gradients in tissue engineering. Tissue Eng Part B Rev 14(4):341–366

Spiegel AM (1996) Genetic basis of endocrine disease. J Clin Endocrinol Metab 81:2434–2442

Tan DCW, Yung LYL et al (2010) Controlled microscale diffusion gradients in quiescent extracellular fluid. Biomed Microdevices 12(3):523–532

Tessier-Lavigne M, Goodman CS (1996) The molecular biology of axon guidance. Science 274(5290):1123–1133

Thorne RG, Hrabetová S et al (2004) Diffusion of epidermal growth factor in rat brain extracellular space measured by integrative optical imaging. J Neurophysiol 92(6):3471–3481

Walker GM, Beebe DJ (2002) A passive pumping method for microfluidic devices. Lab Chip 2(3):131–134

Wang CJ, Li X et al (2008) A microfluidics-based turning assay reveals complex growth cone responses to integrated gradients of substrate-bound ECM molecules and diffusible guidance cues. Lab Chip 8(2):227–237

Wu Z, Jensen H et al (2004) A flexible sample introduction method for polymer microfluidic chips using a push/pull pressure pump. Lab Chip 4(5):512–515

Yoshimoto Y, Imoto M (2002) Induction of EGF-Dependent Apoptosis by Vacuolar-Type H^+-ATPase Inhibitors in A431 Cells Overexpressing the EGF Receptor. Exp Cell Res 279(1):118–127

Zhou J, Ellis AV et al (2010) Recent developments in PDMS surface modification for microfluidic devices. Electrophoresis 31(1):2–16